J. Fluid Mech. (2007), *vol.* 590, *pp.* 497–507.
doi:10.1017/S0022112007008026 Printed in the United Kingdom

Viscosity of a dense suspension in Couette flow

NICOLAS HUANG[1] AND DANIEL BONN[1,2]

[1]Laboratoire de Physique Statistique, École Normale Supérieure, 24 Rue Lhomond, 75231 Paris Cedex 05, France

[2]van der Waals-Zeeman Institute, University of Amsterdam, Valckenierstraat 65, 1018 XE Amsterdam, The Netherlands
daniel.bonn@lps.ens.fr

(Received 17 April 2007 and in revised form 18 July 2007)

We study the rheology of a granular paste, i.e. a dense suspension of non-Brownian particles, quantitatively at steady state, in a cylindrical Couette cell. Previous studies have shown a discrepancy between local and global measurements of the viscosity for these materials, making it impossible to predict their resistance to flow. Using both MRI investigation techniques and classical rheology studies, we show that agreement between local and global measurements can be obtained, provided the migration of particles inside the gap is taken into account. As found by Leighton & Acrivos (*J. Fluid Mech.* vol. 181, 1987, p. 415), the migration leads to a particle density gradient in the flow, the highly sheared regions being less dense in particles. Here, by comparing the local viscosity and particle density measurements from MRI with the macroscopic relation between viscosity and the volume fraction, it is shown that global and local measurements agree with each other. This consequently allows us to define a viscosity for dense suspensions.

1. Introduction

The seemingly simple question of whether a constitutive equation can be defined for granular systems in general does not appear to have a simple answer (GDRMiDi 2004; Jaeger, Nagel & Behringer 1996; Mueth *et al.* 2000), in spite of the fact that it is necessary, for a large number of applications, to predict the resistance to flow. Because of the volume conservation that is not necessarily present for dry granular materials, perhaps the simplest example of granular flow is that of dense suspensions, i.e. pastes or slurries, which are of crucial importance in industrial and civil engineering, and in geophysics, for example, for the understanding of the behaviour of cement, concrete, mudflows, mining slurries, debris flows, lavas, drilling fluids, etc. (Bagnold 1954; Hunt *et al.* 2002; Herminghaus 2005).

For dense suspensions, from the comparison between global (rheological) measurements of the viscosity and local measurements using velocity profiles measured with an MRI (magnetic resonance imaging) scanner, it has been concluded that there is no simple constitutive equation relating shear stress to shear rate only (Huang *et al.* 2005). This is general for granular media, and is the main problem that needs to be solved (Huang *et al.* 2005; GDRMiDi 2004; Jop, Forterre & Pouliquen 2005; Cassar, Nicolas & Pouliquen 2005; Jop, Forterre & Pouliquen 2006). Very recently, a constitutive law for dry dense granular flows has been proposed, following a visco-plastic approach to capture granular flow properties (Jop *et al.* 2006). However, for dense suspensions, no constitutive equation has yet been formulated.

Here we show that for a dense suspension in shear flow, global and local measurements of the viscosity can be made to agree with each other, and that consequently a viscosity can be defined for the granular system. The 'missing link' between the macroscopic and local measurements is found to be the coupling between the flow and the concentration. Flow-induced migration of the particles leads to a concentration gradient in the flow; such particle migration in concentrated suspensions was discovered first by Leighton & Acrivos (1987). Using MRI to measure the gradient in particle density, we find that, due to the flow, the material is dilated where it flows rapidly, and compacted where the flow is slow (Ovarlez, Bertrand & Rodts 2006). This results in a local variation of the viscosity; if this is taken into account, agreement with macroscopic rheology measurements is obtained, thus allowing the viscosity of the dense suspension to be defined.

2. Experimental

We study the rheological behaviour of a granular paste (a dense suspension) composed of non-Brownian spherical monodisperse particles immersed in a Newtonian fluid. The granular material is constituted of spherical monodisperse polystyrene beads (diameter 290 μm $\pm$ 30 μm, density 1.04 g cm^{-3}). We use a Rhodorsil silicone oil as the interstitial fluid (viscosity $\eta_s = 20$ mPa s, density 0.96 g cm^{-3}). The volume fraction is fixed at 58 % for the experiments discussed here. Such a high volume fraction limits sedimentation and creaming effects. Furthermore, the suspensions are strongly pre-sheared before any measurements. In our previous work (Huang *et al.* 2005), careful measurements at density-matched conditions were performed. These measurements provided results that were identical to within the experimental uncertainty with experiments on systems with a slight density mismatch, as is the case of the dense suspensions in this study (polystyrene beads in Rhodorsil oils). With all these precautions (dense suspensions, pre-shear, comparison with previous isodensity data), our data were reproducible and not influenced by spurious density effects.

MRI experiments were performed with a velocity controlled 'MRI-rheometer' from which we directly obtain the local velocity distribution in a Couette geometry (inner cylinder radius $R_i = 4.15$ cm, outer cylinder radius $R_e = 6$ cm; height 11 cm). Magnetic resonance imaging was performed with a Bruker set-up described in detail in Raynaud *et al.* (2002) and Rodts *et al.* (2004). The inner cylinder is driven at velocity Ω_i ranging between 0.01 and 100 r.p.m., corresponding to velocities V_i from 0.004 to 43.5 cm s^{-1}, and to overall shear rates between 0.002 and 23.5 s^{-1}. For technical reasons, Ω_i is either between 0.01 and 9 r.p.m., or between 1 and 100 r.p.m. We pre-shear the material at the maximum rotational speed available ($\Omega_i = 9$ or 100 r.p.m.), for 30 s. As we will explain in detail below, this set-up allows local measurement of the viscosity, as well as the particle concentration in the flowing paste.

Classical rheology experiments are carried out with a vane-in-cup geometry on a commercial rheometer (Reologica Stresstech) that imposes either the stress or the shear rate. The vane geometry is equivalent to a cylinder with a rough lateral surface, with a roughness comparable with the scale of the particles of the sheared granular material itself (Raynaud *et al.* 2002; da Cruz 2004). A rough surface reduces the slipping of granular materials which occurs on smooth surfaces (Larson 1999). For the same reason, the inside of the cup is covered with a layer of granular particles using double-sided adhesive tape. The vane has a diameter of 16 mm and the cup has a diameter of 26 mm. The gap size is therefore 5 mm. For the global measurements, we choose to use a small-gap Couette cell, in order to minimize the effects of the

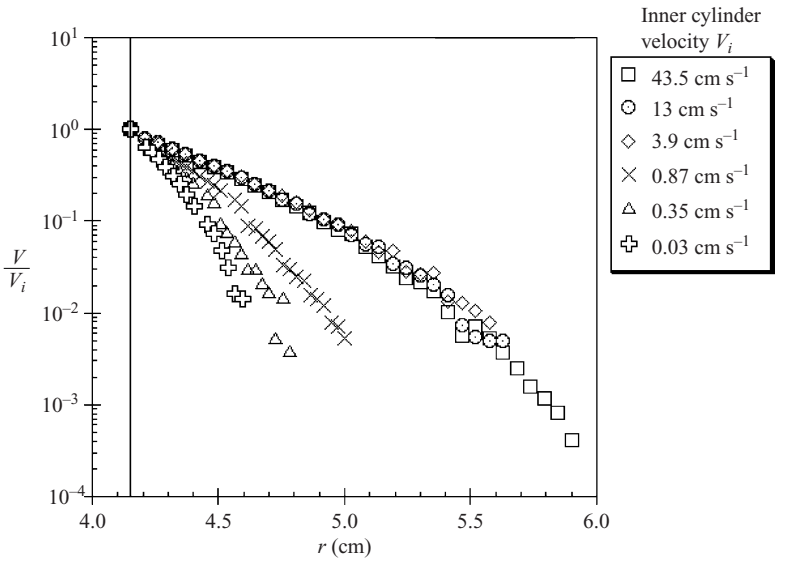

FIGURE 1. Velocity profiles in a Couette geometry at different rotational velocities. The vertical line on the left corresponds to the inner cylinder.

concentration gradient. In two different series of experiments we measure both the stress as a function of the shear rate, and the viscosity as a function of the volume fraction of particles, by preparing pastes with different quantities of beads and silicon oil. Before each experiment, the material is pre-sheared for 30 s at 30 s^{-1} to obtain a reproducible initial state. This set-up allows the measurement of the global viscosity.

3. Results

3.1. *Comparison between global (macroscopic) and local measurements*

We first compare the macroscopic viscosity measurements taken from the small-gap Couette cell to the local measurements. Concentration gradients are usually stronger in a large-gap geometry, leading to a viscosity that decreases in time, and in steady state to a lower viscosity and a highly inhomogeneous material. The viscosity in the small-gap Couette cell did not show a significant time dependence. The local measurements of the viscosity are obtained from the velocity profiles (figure 1) of the flowing granular material in a wide-gap Couette cell inserted in a magnetic resonance imaging (MRI) appparatus. For low velocities (velocities below a critical velocity V_c), only part of the material is sheared. There are then two distinctive bands in the gap: a sheared band and a band where the material is, to within the experimental accuracy, motionless. This is a direct observation of shear banding in our granular material.

In these MRI measurements, if we suppose that our material is a homogeneous continuum medium, the shear stress varies within the gap, and the stress σ at a given radial position r as a function of both the applied torque C and the fluid height h follows from momentum balance. Note that the MRI shear cell does not allow measurement of the stress. To measure the stress at $r = R_i$, a classical shear cell of the same size as the MRI cell is used. The same velocities as in the MRI experiments are applied to the inner cylinder, and the corresponding stresses on this cylinder σ_i are measured.

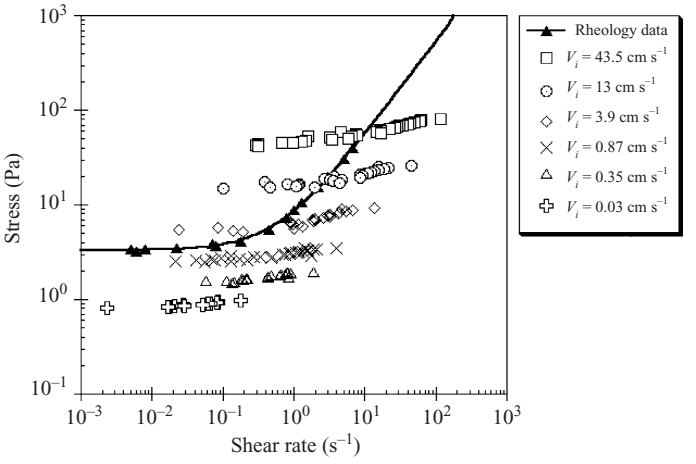

FIGURE 2. Flow curves (shear stress versus shear rate) calculated from the velocity profile and measured macroscopically. The paste has a volume fraction ϕ of 58 %. The value of the shear rate $\dot{\gamma}$ in the macroscopic experiment (rheology data) is taken at $r = R_i$. On the macroscopical curve there is a horizontal plateau at low shear rates. The macroscopic (global) measurements are taken from the small-gap Couette cell, in order to minimize the effects on the concentration gradient.

We can reasonably assume that, even though granular force chains should be present in the sheared granular system, momentum conservation is likely to hold, at least on average. Therefore, the momentum balance equation gives the local stress in the MRI cell as

$$\sigma = \sigma_i \frac{R_i^2}{r^2}. \tag{3.1}$$

The magnitude of the shear rate can be deduced from the velocity profile $v_\theta(r)$ as, in a cylindrical Couette cell,

$$\dot{\gamma} = r \frac{\partial}{\partial r}\left(\frac{v_\theta}{r}\right). \tag{3.2}$$

Thus r can be eliminated from these two equations to deduce the constitutive equation of the fluid in simple shear, i.e. the relation between σ and $\dot{\gamma}$.

The local and global flow curves are plotted in figure 2, and show that, first, the data are not consistent between different MRI experiments, and second, they are very inconsistent with the rheology data (Huang *et al.* 2005). On the macroscopic flow curve, note the presence of a horizontal plateau at low shear rates. This precludes the existence of a simple constitutive equation relating shear stress to shear rate only. These results can be understood if we combine the momentum balance equation with the roughly exponential decay of the velocity profile, and calculate a local viscosity from the ratio of the two. It then follows that this local viscosity is small near the moving inner cylinder, and increases with increasing distance from the moving wall. Since in these dense granular systems the viscosity is strongly dependent on the particle concentration, this suggests that the particle concentration is slightly smaller near the moving wall where the shear rate is the highest, and slightly larger near the stationary wall, where the shear rate is very small. Because of the inhomogeneity, the material is not necessarily the same throughout the gap: the particle density may vary. To see whether this is indeed true, we will calculate the spatial variation of the viscosity from the MRI data, and measure the spatial variation of the particle volume

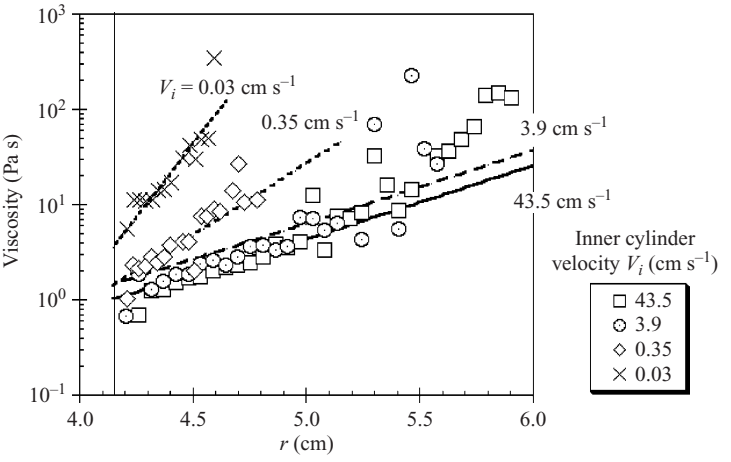

FIGURE 3. Viscosity inside the gap (MRI cell). The lines correspond to the exponential fit to the velocity profiles. The symbols correspond to the data taken from the velocity profiles. The paste has a volume fraction ϕ of 58 %. The vertical line on the left corresponds to the inner cylinder.

fraction, also with the MRI. These results can then be compared to macroscopic measurements of the volume-fraction dependence of the viscosity.

3.2. *Viscosity profiles inside the gap*

The viscosity profiles inside the gap can be computed directly from the velocity profiles of figure 1. We previously found that the velocity profiles can be collapsed onto a single universal curve with the rescaled coordinates V/V_i and $(r - R_i)/d_c$, where d_c is the extent of the material that is sheared (Huang *et al.* 2005). A fit gives

$$\frac{V}{V_i} = \exp\left(-\alpha \frac{r - R_i}{d_c(V_i)}\right), \tag{3.3}$$

with $\alpha = 5.6$ (Huang *et al.* 2005); $\dot{\gamma}(r)$ can be obtained from this equation and from (3.2). It follows that

$$\dot{\gamma}(r) = V_i \left(\frac{\alpha}{d_c} + \frac{1}{r}\right) \exp\left(-\alpha \frac{r - R_i}{d_c}\right). \tag{3.4}$$

Finally, using (3.1), the viscosity $\eta(r) = \sigma(r)/\dot{\gamma}(r)$ inside the gap is

$$\eta(r) = \frac{\sigma(r)}{\dot{\gamma}(r)} = \frac{R_i^2}{r} \frac{d_c}{d_c + \alpha r} \frac{\sigma_i}{V_i} \exp\left(\alpha \frac{r - R_i}{d_c}\right). \tag{3.5}$$

If $V \geqslant V_c$ ($V_c \approx 1\,\mathrm{cm\,s^{-1}}$ being the critical velocity), the whole gap is sheared and $d_c = e = 1.85\,\mathrm{cm}$ (Huang *et al.* 2005). V_c is thus the critical rotation velocity above which no shear banding is observed. For $V < V_c$, $d_c(V_i)$ shows a power-law behaviour with an exponent $n_{d_c} = 0.43$.

Figure 3 shows the viscosity profiles $\eta(r)$ inside the gap. The experiments thus show that if no shear banding is observed (i.e. $V \geqslant V_c$), the velocity profiles for different speeds are very similar. On the other hand, if shear banding is observed, the viscosity profiles are significantly above those taken for V greater than V_c.

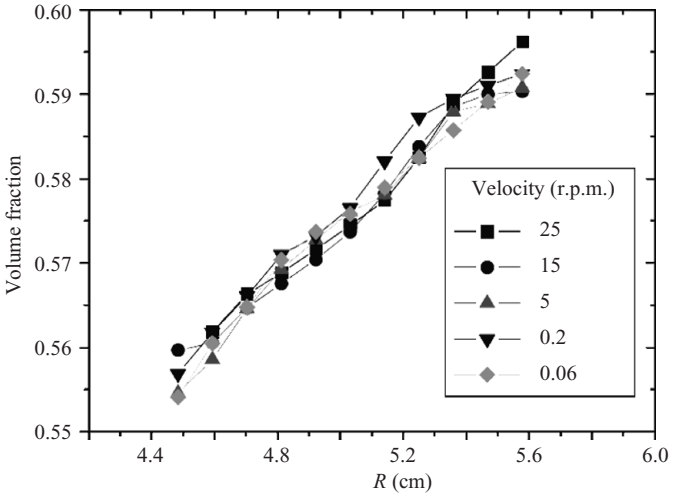

FIGURE 4. Density profile of the paste in the gap of the MRI Couette cell for different rotation speeds of the inner cylinder (Ovarlez *et al.* 2006). The paste has a volume fraction ϕ of 58 %.

3.3. *MRI measurements of the density profile inside the gap*

The results from the viscosity profiles therefore show that the viscosity is lower near the moving inner cylinder, and higher at the stationary outer wall. This suggests that a density gradient develops in the flow. We therefore measured the concentration profile with the MRI scanner; at the chosen frequency, the MRI is only sensitive to the protons present in the silicon oil (not in the polystyrene beads), and the MRI signal is directly proportional to the proton density (Ovarlez *et al.* 2006). By a careful calibration with only the silicon oil, the volume fraction of beads can be obtained directly throughout the gap of the Couette cell, with a resolution similar to that for the velocity profiles.

Figure 4 shows the measured density profiles for different rotation speeds of the inner cylinder. A surprising observation is that the density profiles are the same to within the experimental accuracy for different rotation speeds. This is most likely to be due to the pre-shear: the density profile is established after the pre-shear (as shown with the MRI), and does not change significantly thereafter. This seems reasonable for the smallest rotation rates; however, the pre-shear having been at 9 r.p.m., for the rotation rates of 15 and 25 r.p.m. one might have expected a larger gradient. The data, again taken in steady state, therefore suggest that for high enough rotation rates the density profile no longer changes with the rotation rate. No changes in the density profiles were observed, even after after several hours (Ovarlez *et al.* 2006). These authors show that the density profile is irreversibly established by the pre-shear and even observe the same concentration profile for a 9 r.p.m. pre-shear as for a 100 r.p.m. pre-shear (Ovarlez *et al.* 2006). Comparing our results to those of Leighton & Acrivos (1987) is difficult, since they discuss the shear-induced migration out of the gap into a particle reservoir. In the MRI Couette cell there is also a reservoir (below the rotating inner cylinder), but the observation that the density profiles are independent of the macroscopically imposed rotation rate shows that this effect is negligible for our experiments. This does not however rule out a migration from the gap into the reservoir during the pre-shear. However the observation that the average concentration measured with the MRI remains close to the 58 % volume

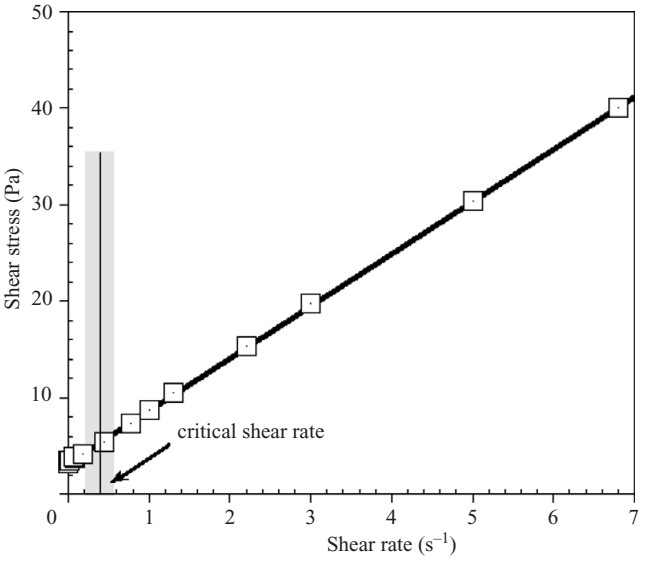

FIGURE 5. Flow curve (shear stress versus shear rate) at an imposed macroscopic shear rate in a linear–linear scale, with a linear fit. The paste has a volume fraction ϕ of 58 %. For the stress range we are interested in here (above the critical stress), the viscosity can be considered as constant. The shaded area is the statistical error bar for the critical stress.

fraction that was the initial state of the sample shows that this effect, if present, is too small to be detected experimentally by the MRI.

More importantly for our purposes, the density profiles show that the particle concentration is lowest near the moving wall, and increases roughly linearly within the gap of the Couette cell. This is in qualitative agreement with the assumption that the viscosity variation in the gap is indeed due to a gradient in particle concentration. This link will be made quantitative below, by measuring the viscosity as a function of the volume fraction of particles.

3.4. *Viscosity as a function of the volume fraction: Krieger–Dougherty equation*

The measurements of the flow curve (figure 5) show that, on a linear–linear scale, the paste behaves almost as a Newtonian fluid; deviations from this are important at very low shear rates due to the finite yield stress of the paste. However, for most of the shear rate range we are interested in here, the viscosity can reasonably be taken constant, i.e. independent of the shear rate.

This viscosity does depend very strongly on the volume fraction of particles: figure 6 shows a comparison between the measured global viscosity and the well-known Krieger–Dougherty model for the dependence of the viscosity η_s on the volume fraction ϕ:

$$\eta = \eta_s \left(1 - \frac{\phi}{\phi_m}\right)^{-2.5\,\phi_m}, \tag{3.6}$$

with η_s the solvent viscosity and ϕ_m the random close packing (Krieger & Dougherty 1959; Larson 1999). This phenomenological model provides us with a good description of the data. We can therefore use this model, together with the results from the density profile, to recalculate the viscosity distribution in the large-gap Couette cell used for the velocity and density profile measurements.

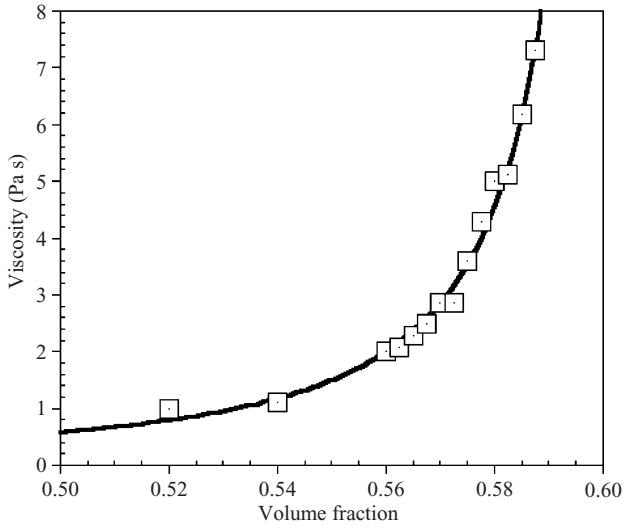

FIGURE 6. Global viscosity versus volume fraction (gap size 5 mm) with a fit from the Krieger–Dougherty model. The fit gives $\phi_m = 60.8 \pm 0.1\,\%$.

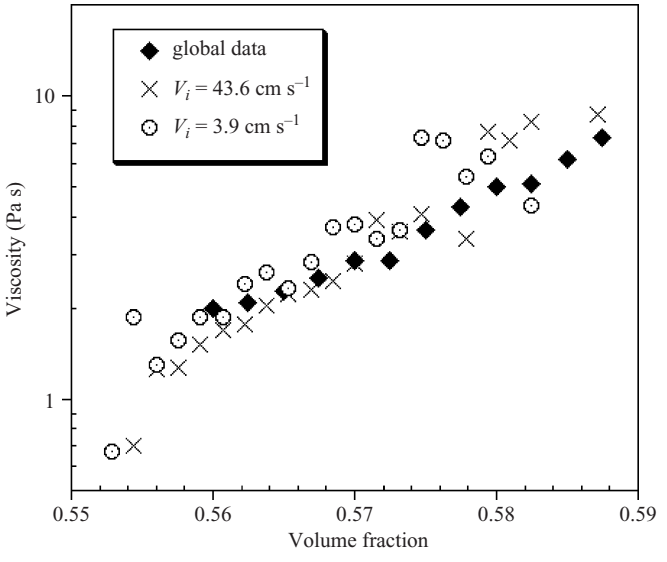

FIGURE 7. Comparison between global and local measurements, with the volume fraction inside the gap taken into account.

3.5. *New comparison between global and local measurements*

We are now in a position to quantitatively compare the results from the local and global measurements of the viscosity. For the local measurements, we take into account the particle density gradient by defining $\sigma = \eta(\phi)\dot{\gamma}$, with $\eta(\phi)$ depending on the volume fraction ϕ. $\eta(\phi)$ follows the Krieger–Dougherty model (3.6) discussed above, and ϕ increases linearly with r inside the gap.

The previous result for global measurements is compared to the local measurements in figure 7, and the agreement between local and global measurements is now very satisfactory for inner-cylinder velocities above the critical velocity, in order for the

whole gap to be sheared. The lower rotation velocities are discussed in § 4. For this quantitative comparison, we also need to know the wall shear stress in the Couette geometry; there is some uncertainty in this value due to residual sedimentation effects. This, however, only leads to a vertical translation of the MRI results and does not change the overall shape of the flow curve. The good agreement therefore allows a definition of the viscosity for our dense suspension in a steady-state shear flow. Furthermore, the agreement shows that measurements in a small-gap Couette cell allow the material and its viscosity to be characterized accurately. This is very likely because a small gap minimizes, or even suppresses, the particle concentration gradient: particle migration towards the outer cylinder leads to a viscosity decrease (Leighton & Acrivos 1987). The good global–local agreement is likely to be due to the fact that a density gradient cannot be fully developed, in a small-gap Couette geometry. This is because the basic mechanism behind the migration is that gradients in shear rate generate a particle flux towards the outer cylinder, which is counterbalanced by a particle flux due to viscosity gradients. In a small-gap, large-aspect-ratio Couette cell such as the one used here, the shear rate gradient is very small, and one may therefore expect that the migration is also small. Experimentally, the gradient, if present in the small gap, is not noticeable in our viscosity experiments. Thus, the local measurements show the pertinence of measurements in gaps wide enough to have a continuous flow (gap size of several bead diameters), but small enough to minimize migration effects.

4. Discussion

We have shown that a constitutive equation can be defined for a dense suspension in a steady-state Couette flow. The flow of the dense suspension is governed by the flow curve equation $\sigma = \eta(\phi)\dot{\gamma}$. The viscosity $\eta(\phi)$ depends on the volume fraction ϕ, and their relationship follows the Krieger–Dougherty model: $\eta = \eta_s(1 - \phi/\phi_m)^{-2.5\,\phi_m}$. It follows from the data that the particle volume fraction increases linearly with increasing distance from the moving inner cylinder, which, quantitatively and with a rheological investigation inside the gap (local measurements), confirms the idea that the viscosity varies within the gap due to a flow-induced density gradient (particle migration) (Gadala-Maria & Acrivos 1980; Leighton & Acrivos 1987; Abbott *et al.* 1991; Phillips *et al.* 1992; Wolthers *et al.* 1996). This result is deducted from density profiles, viscosity profiles (deduced from experimental velocity profiles), and from the comparison between local and global measurements (the latter performed in a small-gap cell).

The method described in this paper still relies on the (difficult) measurement of the density profile, and is therefore neither predictive, nor directly applicable to other flow situations, as is necessarily the case for a 'real' constitutive equation. For instance, segregation phenomena similar to those observed here but resulting from a competition between gravity and shear have recently been observed in other (non-isodense) dense suspensions, see Barentin, Azanza & Pouligny (2004) and Lenoble, Sabre & Pouligny (2005). In our experiments however, sedimentation effects are negligible and the particle migration is induced by the shear. Our way of defining a viscosity should be applicable to both situations, as long as the concentration gradient is known or can be measured, and the problem of particle migration appears to be one that is much easier to tackle than that of the prediction of flow of granular materials in general. However, the mechanisms of shear-induced migration are not fully understood, perhaps because quantitative measurements of the density profiles are also difficult to make. Ovarlez *et al.* (2006) have studied the dynamics of migration

in detail in our system, and conclude that the dynamics is much faster than would be expected from theoretical models for shear-induced migration, the reason for which remains unclear for the moment. In our study, the dynamics of migration does not influence the results as it is in steady state.

Very recently, Lagrée & Lhuillier (2006) proposed a continuum-mechanical description for the flow of dense suspensions in a Couette cell. They consider exactly our experimental situation, and determine the density profile resulting from a competition between dilatancy and particle diffusion due to a gradient in suspension viscosity, brought about by a gradient in concentration. The density profile is determined in their work for a constant confining pressure, and they found that the radius dependence may be somewhat weaker than the approximately linear behaviour observed experimentally. Our experiments however were done at constant volume fraction rather than at constant pressure. Their subsequent work (Lagrée & Lhuillier 2006, personal communication) however shows that the form of the density profiles is virtually unchanged when a constant volume fraction is imposed, as is the case in the experiments. A quantitative comparison is in progress.

It should also be noted that for low velocities V_i, and notably whenever shear banding occurs, our method does not allow a viscosity to be defined that is identical for global and local measurements. Since the concentration profiles do not depend on V_i, this follows directly from the observation that the viscosity profiles $\eta(r)$ do not coincide. In the region where no flow occurs, the velocity is zero (figure 2), and consequently the viscosity infinite. Thus, localization of the flow is the first reason why the viscosity profiles do not coincide.

The second reason is more subtle. The macroscopic flow curve (figure 2) shows that, to a good approximation, the fluid behaviour is Newtonian at higher rotation speeds. This approximation breaks down for $V_i < V_c$. For these low rotation rates, the non-zero intercept (yield stress) in figure 6 contributes also significantly to the viscosity of the flowing part, and as a result the viscosity is higher. More quantitatively, for this Bingham fluid, when $V_i = 0.03\,\mathrm{cm\,s^{-1}}$ (for example), the sheared region has an extent d_c of $0.5 \pm 0.06\,\mathrm{cm}$. The corresponding shear rate is therefore $\dot{\gamma} = V_i/d_c = 0.06 \pm 0.01\,\mathrm{s^{-1}}$. The shear stress is $\sigma_i = 1.5$ Pa. Hence the mean viscosity for a Bingham fluid: $\eta_b = \sigma_i/\dot{\gamma} \approx 25\,\mathrm{Pa\,s}$. Supposing that the fluid is Newtonian, a direct fit to the rheology data (figure 2) gives a mean viscosity for a Newtonian fluid of $\eta_n \approx 5\,\mathrm{Pa\,s}$. There is consequently a difference of a factor of about 5 between the viscosities of the Newtonian and Bingham models, which can be seen in the viscosity profiles of figure 3. Thus, the fact that at very low speed the fluid should be considered as a Bingham fluid, and not as a Newtonian fluid, is the second reason why the viscosity profile $\eta(r)$ is not independent of the rotation speed V_i, and thus the two viscosities (inside and outside the shear band) are different.

We thank G. Ovarlez, F. Bertrand and S. Rodts for help with the MRI experiments, and D. Lhuillier, B. Pouligny and P.-Y. Lagrée for very helpful discussions. The LPS of the ENS is an UMR 8550 of the CNRS, associated with the universities Paris 6 and Paris 7.

REFERENCES

Abbott, J. R., Tetlow, N., Graham, A. L., Altobelli, S. A., Fushima, E., Mondy, L. A. & Stephens, T. S. 1991 A constitutive equation for concentrated suspensions that accounts for shear-induced particle migration: Couette flow. *J. Rheol.* **35**.

Bagnold, R. A. 1954 Experiments on a gravity-free dispersion of large solid spheres in a newtonian fluid under shear. *Proc. R. Soc. Lond.* **225**, 49–63.

Barentin, C., Azanza, E. & Pouligny, B. 2004 Flow and segregation in sheared granular slurries. *Europhys. Lett.* **66**, 139–145.

Cassar, C., Nicolas, M. & Pouliquen, O. 2005 Submarine granular flows down inclined planes. *Phys. Fluid Mech.* **17**, 103301.

da Cruz, F. 2004 Écoulement de grains secs : frottement et blocage. PhD thesis, École Nationale des Ponts et Chaussées, Marne-la-Vallée.

Gadala-Maria, F. & Acrivos, A. 1980 The avalanching of granular solids on dune and similar slopes. *J. Rheol.* **24**, 799–814.

GDRMiDi 2004 On dense granular flows. *Eur. Phys. J.* E **14**, 341–365.

Herminghaus, S. 2005 Dynamics of wet granular matter. *Adv. Phys.* **54**, 221–261.

Huang, N., Ovarlez, G., Bertrand, F., Rodts, S., Coussot, P. & Bonn, D. 2005 Flow of wet granular materials. *Phys. Rev. Lett.* **94**, 028301.

Hunt, M. L., Zenit, R., Campbell, C. S. & Brennen, C. E. 2002 Revisiting the 1954 suspension experiments of r. a. bagnold. *J. Fluid Mech.* **452**, 1–24.

Jaeger, H. M., Nagel, S. R. & Behringer, R. P. 1996 Granular solids, liquids, and gases. *Rev. Mod. Phys.* **68**, 1259.

Jop, P., Forterre, Y. & Pouliquen, O. 2005 Crucial role of side walls for granular surface flows: consequences for the rheology. *J. Fluid Mech.* **541**, 167–192.

Jop, P., Forterre, Y. & Pouliquen, O. 2006 A constitutive law for dense granular flows. *Nature* **441**, 727–730.

Krieger, I. M. & Dougherty, T. J. 1959 A mechanism for non-Newtonian flow in suspensions of rigid spheres. *Trans. Soc. Rheol.* **3**, 137–152.

Lagrée, P.-Y. & Lhuillier, D. 2006 The Couette flow of dense and fluid-saturated granular media. *Eur. J. Mech. B-Fluids* **25**, 960–970.

Larson, R. G. 1999 In *The Structure and Rheology of Complex Fluids*. Oxford University Press.

Leighton, D. & Acrivos, A. 1987 The shear-induced migration of particles in concentrated suspensions. *J. Fluid Mech.* **181**, 415–439.

Lenoble, M., Sabre, P. & Pouligny, B. 2005 The flow of a very concentrated slurry in a parallel-plate device: Influence of gravity. *Phys. Fluids* **17**, 073303.

Mueth, D. M., Debregeas, G. F., Karczmar, G. S., P. J. Eng, S. R. Nagel & Jaeger, H. M. 2000 Signatures of granular microstructure in dense shear flows. *Nature* **406**, 385–389.

Ovarlez, G., Bertrand, F. & Rodts, S. 2006 Local determination of the constitutive law of a dense suspension of non-colloidal particles through MRI. *J. Rheol.* **50**, 259.

Phillips, R. J., Armstrong, R. C., Brown, R. A., Graham, A. L. & Abbott, J. R. 1992 A constitutive equation for concentrated suspensions that accounts for shear-induced particle migration. *Phys. Fluids* A **4**, 30–40.

Raynaud, J. S., Moucheront, P., Baudez, J. C., Bertrand, F., Guilbaud, J. P. & Coussot, P. 2002 Direct determination by nuclear magnetic resonance of the thixotropic and yielding behavior of suspensions. *J. Rheol.* **46**, 709–732.

Rodts, S., Bertrand, F., Jarny, S., Poullain, P. & Moucheront, P. 2004 Développements récents dans l'application de l'IRM á la rhéologie et á la mécanique des fluides. *C. R. Chimie* **7**, 275–282.

Wolthers, W., van den Ende, D., Duits, M. H. G. & Mellema, J. 1996 The viscosity and sedimentation of aggregating colloidal dispersions in a Couette flow. *J. Rheol.* **40**, 55–67.